Status of the NA48 experiment at the CERN SPS

E. Mazzucato[a]

[a]CE Saclay, DSM/DAPNIA,
F-91191 Gif-sur-Yvette Cedex, France

The installation of the NA48 detector has been completed in 1996 with the commissioning of the liquid krypton electromagnetic calorimeter. Preliminary results from a test run performed at nominal beam intensity indicate that the NA48 detector works according to expectations.

1. INTRODUCTION

The NA48 experiment at the Cern SPS aims at measuring the direct CP violation parameter $\Re(\epsilon\prime/\epsilon)$ with a precision of about 2×10^{-4} [?] by comparing the relative decay rates of short- and long-lived kaons into two neutral or two charged pions:

$$\frac{\Gamma(K_L^0 \to \pi^0\pi^0)}{\Gamma(K_S^0 \to \pi^0\pi^0)} \Big/ \frac{\Gamma(K_L^0 \to \pi^+\pi^-)}{\Gamma(K_S^0 \to \pi^+\pi^-)} \cong 1 - 6\Re(\epsilon\prime/\epsilon).$$

The principle of the experiment consists in collecting the four relevant decay modes concurrently in the same detector, using almost collinear K_L and K_S beams distinguished by tagging the proton which produces the K_S particle. In this way, differences and variations in detection efficiencies for K_S and K_L decays become unimportant, as do rate dependent effects introduced by accidental activity in the detector elements.

High-rate capability and high-resolution detectors for the identification of the charged and neutral pion modes and for the proton tagging system are necessary to provide excellent background rejection and to keep the systematical uncertainties at the desired level.

2. EXPERIMENTAL SET-UP

A schematic view of the kaon beam lines and of the detector layout is shown in Figure 1. A 450 GeV/c primary proton beam with a nominal flux of 1.5×10^{12} particles per pulse (ppp) impinges on a Be target at a downward angle of 2.4mrad to produce the neutral K_L beam. A dipole magnet located downstream of the target station sweeps away the emitted charged particles and deflects the remaining primary protons towards a Si bent crystal. A small fraction ($\approx 5\times10^{-5}$) of these protons are channelled by the crystal and deflected back onto the K_L beam line after passing through a tagging detector. All other charged particles are absorbed in a beam dump.

The resulting low-intensity ($\approx 3\times10^7$ ppp) proton beam is then transported towards a second Be target for the production of the short-lived kaons. The K_S target is positioned 72mm above the K_L beam axis and 109m downstream of the bent crystal. The proton beam strikes the K_S target at an angle of 4.2mrad. This production angle is chosen in order to render the momentum spectrum of the detected K_S as similar as possible to the K_L one over the 70-170GeV/c study range.

The K_S target is followed by a sweeping dipole magnet and a 6m long collimator which defines a K_S beam that converges towards the NA48 detector at a downward angle of 0.6mrad. The end of the K_S collimator coincides with the last of a series of three defining collimators for the K_L beam. Thus, K_L and K_S decays can be produced simultaneously in almost identical fiducial volumes.

The investigated decay region has a length of about 18m ($3\tau_S$) and the corresponding ratio of K_S to K_L decays into two pions is about 3. The beginning of the kaon decay region is precisely defined by an anticounter which detects all decays occuring upstream. The decay volume lies inside a large, 90m long vacuum tank covered with seven rings of scintillation counters to reject $K_L \to 3\pi^0$ decays. It is terminated by a thin kevlar window.

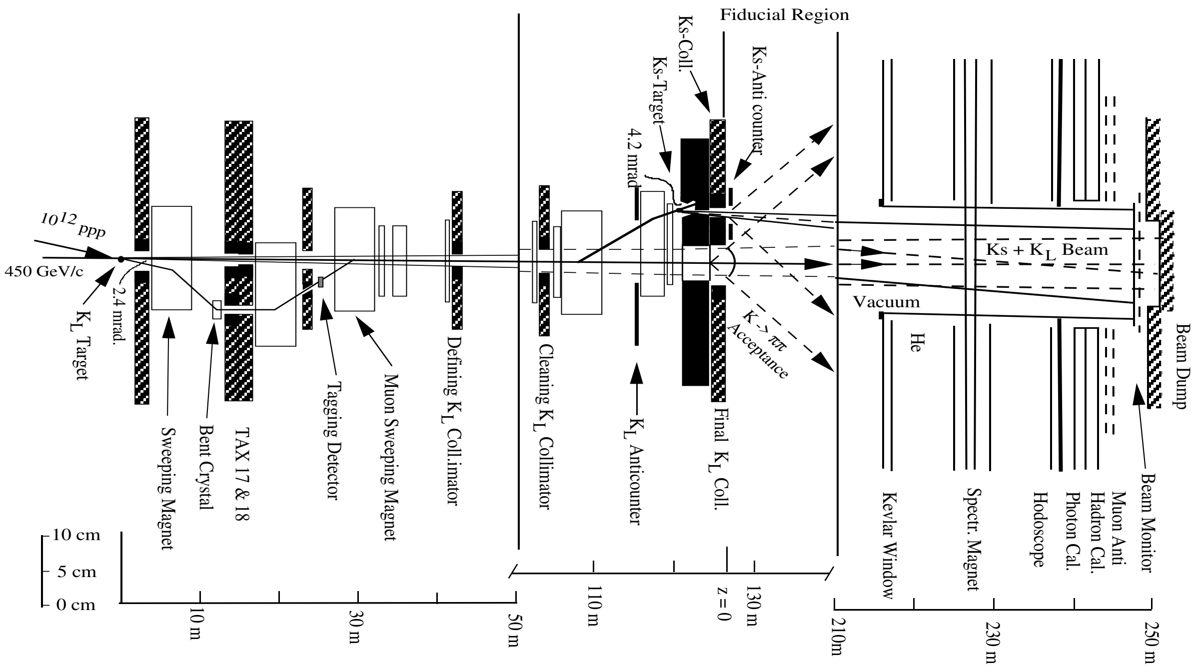

Figure 1. The NA48 Kaon beams.

The decay volume is followed by the NA48 detector which extends from a distance of 216m to 255m downstream of the K_L target. It consists of a magnetic spectrometer contained in a helium tank made of stainless steel and closed by a 4mm thick aluminum endcap, a scintillator hodoscope counter for triggering on charged decays, a photon detector followed by a hadronic calorimeter and a muon veto detector. A vacuum beam pipe with a 160mm diameter traverses all the detector elements to let the neutral beam go through.

3. THE NA48 DETECTOR

The NA48 detector has been designed to identify neutral kaon decays with excellent energy, position and time resolutions at rates exceeding 1MHz. The main components of the NA48 detector are described in this section.

3.1. The proton tagging counter

The knowledge of the origin of a decay in the K_L or K_S beam relies on the information provided by the tagging counter located upstream of the K_S target. The K_L or K_S assignment is obtained by measuring the time difference between the passage of the proton in the tagging counter and the event time in the detector. Events with a time difference inside a given interval are called "K_S", any other events are called "K_L". Inefficiencies in the tagging counter such as misalignment and deadtime cause K_S decays to be identified as K_L. On the other hand, any accidental hit in the tagging counter produces a K_L to K_S transition. Since these misidentifications are decay-mode independent, they only lead to a dilution of $\Re(\epsilon\prime/\epsilon)$.

The proton tagging detector has been designed to cope with proton rates above 10MHz and to provide a detection efficiency close to 100% combined with a time resolution better than 500ps[?]. It consists of two sets of twelve staggered scintillator foils arranged alternately in the horizontal and vertical directions. All foils have a thickness of 4mm. The width of the foils vary between 200μm near the beam axis up to 3000μm for the scintillators located at the beam edges so that each counter sees only a fraction of the beam. To ensure excellent geometrical efficiency, an overlap of 50μm is kept from one counter to the next one in each projection. The horizontal foils are made of NE-102a scintillator whereas the vertical ones are made of BC-418 scintillator.

The scintillator foils are mounted on a carbon fiber support structure which has a mechanical precision better than 40μm. The scintillation light is transmitted to R-2076 Hamamatsu photomultipliers via alumnized mylar envelopes and lucite light guides. The light yield obtained with beam particles varies between 300 and 400 photoelectrons.

The precise positioning of the tagging system with respect to the beam axis is achieved by using four independent remote-controlled motors for horizontal and vertical displacements and for rotations around the horizontal and vertical axis. Alignment accuracy of 200μrad can be reached during beam scans by looking at the tagger multiplicity distribution normalized to the number of protons that hit only one counter.

The signals of the individual counters are digitized by two 8-bit 480Mz FADC chips running in interleaved mode. The average time resolution of a single counter was measured to be about 180ps and the double-pulse separation is below 5ns, yielding at 20MHz a dead time of less than 1% for the proton detection. Figure 2 shows the time difference distribution of two horizontal counters when the tagging counter is slightly tilted to let the proton beam hit several foils.

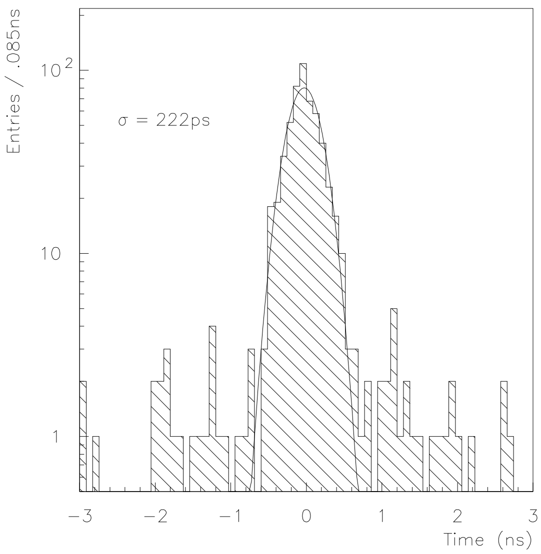

Figure 2. Time difference distribution between tagging counters H1 and H2.

3.2. The magnetic spectrometer

The identification of $K_{L,S} \rightarrow \pi^+\pi^-$ decays is performed using a high-resolution magnetic spectrometer which consists of a dipole magnet and a set of four drift chambers. The magnet has an aperture of 2.45$\times$2.4m^2 and produces a maximum magnetic field of 3.7kGauss in the vertical direction. The transverse momentum kick at the center of the magnet is 256MeV/c. Two drift chambers are located upstream of the magnet for the measurement of the decay vertex position whereas the other two, located dowstream of the magnet, are used for the bending angle determination of the tracks. To reduce multiple scattering effects, the entire spectrometer is contained in a large tank filled with helium at atmospheric pressure. The total length of the spectrometer is about 22m.

The four drift chambers have an octagonal shape with a transverse dimension of 2.9m. Each chamber contains eight planes of grounded sense wires oriented in four different directions orthogonal to the beam axis: 0° (X,X′), 90° (Y,Y′), −45° (U,U′) and +45° (V,V′). The electric field is produced by two field wire planes located on each side of the sense wire plane at a distance of 3mm. The spacing between two wires, both on the field and the sense wire planes, is 1cm so that the maximum transverse drift distance in a cell is 5mm. One view contains two staggered sense planes distant by 12mm along the beam axis. It is isolated from the next view by two 22μm thick graphite coated mylar foils placed at a $\pm$24mm distance from the center plane of the view.

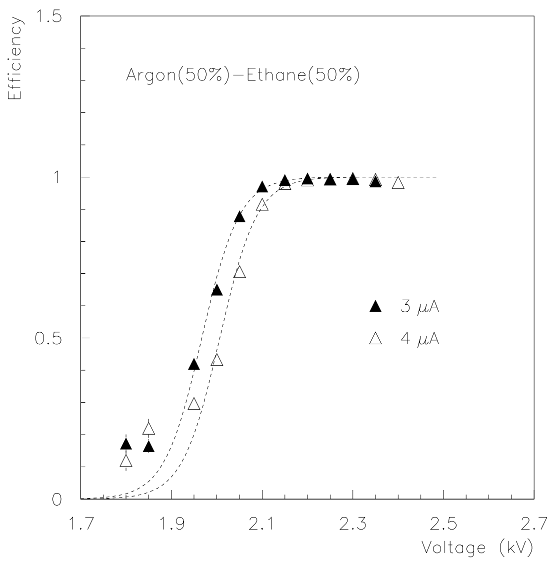

Figure 3. Drift chamber efficiency plateau.

The mylar foils are connected to high voltage and are used to reduce the electric field intensity on the field wires. The sense wires have a diameter of 20μm and are made of gold plated tungsten while the field wires have a diameter of 120μm and are made of gold plated copper-titanium. One sense wire plane contains 256 wires and the total number of wires in a chamber is 6160.

During the construction of the chambers, care was taken in order to guarantee a precise positioning of the wires on the chamber frames. The absolute transverse position of the wires is known to better than 100μm/m while the 1cm gap between two wires is achieved to better than 10μm (rms) and the the parallellism of the wires is better than 25μm/m (rms). Additional details on the construction of the drift chambers can be found elsewhere[?].

The drift chambers are operated with a standard Argon(50%)-Ethane(50%) gas mixture with a small addition of water vapour ($\leq$1%) to slow down aging processes. The high voltage applied to the field wires and the mylar foils is respectively -2250V and -1405V. The gas gain obtained with these operation conditions is about 6×10^4.

Each sense wire is connected to ground via a preamplifier circuit which has a gain of about 30mV/μA and a rise time of 18ns. Signals are discriminated and then digitized by a 40MHz TDC with a 25/16ns fine time and a 204.8μs memory ring buffer. The detection efficiency achieved with a discrimination threshold of 3μA is measured to be better than 99% in each plane. Figure 3 shows the efficiency dependence on the applied high voltage for two different current thresholds.

The space resolution obtained with these chambers is about 120μm in each projection (X or Y) and is almost insensitive to the beam intensity. The track momentum resolution is given by

$$\frac{\sigma_P}{P}(\%) = .47 \oplus .011P[GeV/c].$$

The thickness of a chamber corresponds to $4.3\times10^{-3}X_0$ while the total contribution from the helium gas contained in the tank is about $4\times10^{-3}X_0$.

3.3. The charged hodoscope

The precise time reference of a $K_{S,L} \to \pi^+\pi^-$ decay is provided by two planes of 64 horizontal and 64 vertical NE-110 scintillator counters. These counters have a width of 6.5cm and a thickness of 2cm. The time resolution of an individual counter is better than 400ps yielding thus a time resolution of better than 200ps for a two-pion event.

3.4. The electromagnetic calorimeter

The detection of the π^0 decay photons is a crucial part of the experiment. In order to meet the precision requirements for the $\Re(\epsilon\prime/\epsilon)$ measurement, the electromagnetic calorimeter must have excellent energy resolution as well as good space resolution and fine granularity for the rejection of the overwhelming $K_L \rightarrow 3\pi^0$ background. In addition, the photon detector must perform reliably at rates of the order of 1MHz and must provide a time resolution better than 1ns to cope with the rate of the tagging counter.

The electromagnetic calorimeter which has been designed for the NA48 experiment consists in a quasi-homogeneous liquid krypton (LKr) detector with a 2×2cm^2 longitudinal tower structure. Its transverse dimension is about 2.6m and its thickness is 125cm, corresponding to about 27X$_0$ of liquid krypton. The calorimeter has also a projective geometry with a maximum aperture angle of 10mrad. The density of the liquid krypton is 2.41g/cm^3 at T=120°K, the Moliere radius is 4.7cm and the radiation length is 4.7cm. The total krypton volume in the cryostat is about 10m^3.

The electrodes are made of 40μm thick copper-beryllium ribbons oriented along the beam axis. They have a width of 18mm and are attached at both ends by a front-plate and a back-plate made of Stesalit 4411W. The position accuracy of the electrodes inside the calorimeter is insured by five 5mm thick Stesalit plates with 10mm×18.5mm holes to let the ribbons go through. These slot masks have been precisely machined to guarantee a local accuracy in the positioning of the ribbons better than 50μm and an absolute transverse position better than 100μm/m. In addition, they are alternatively displaced by +/-50mrad with respect to the beam axis in order to produce a zig-zag geometry of the cells. This feature provides a good mechanical positioning of the ribbons and allows to smear signal losses when particles impinge very close to the electrodes location. The amount of passive material in front of the calorimeter is about .85X$_0$.

The drift cell size is defined by a central anode and by two cathodes at a distance of 10mm on each side of the anode. A 2mm gap separates adjacent layers of cells in the vertical direction. Figure 4 shows a schematic view of the calorimeter electrode structure.

To achieve excellent energy resolution and speed, the initial current read-out technique is used. Signals collected from each anode are sent to preamplifiers located on the back-plate, in the liquid krypton. These are silicon JFET charge integrating amplifiers with a restoring time of 150ns. The signals are then differentiated outside the calorimeter by transceivers located directly on feedthroughs and sent via twisted-pair cables to a shaping amplifier, 10m away. The shaping amplifier output signal has a width of 80ns and a 3% undershoot which lasts few microseconds corresponding to the drift time of electrons across the cell. To efficiently cover a dynamical range of 3.5MeV to 50GeV for the energy deposited in a single cell, a 4-gain switching amplifier is used with respective gains of 1, 2.9, 7.1 and 17.7. The output signals of the shaper amplifiers are digitized by 10-bit FADCs running at 40MHz in a fully pipeline mode.

To improve the time measurement of the detected photons, scintillator fibers have been inserted vertically in the liquid krypton at a depth of 9.5X$_0$. The fibers have a diameter of 1mm and are ganged in bundles of about 25. These are accurately positioned between ribbons. The scintillator fibers are instrumented with Hamamatsu-1355 photomultipliers also located in the liquid krypton. The time resolution achieved with these scintillator counters is better than 250ps.

The performance of such a calorimeter has been recently measured with a prototype [?]. The energy resolution achieved with an electron test beam is

$$\frac{\sigma_E}{E} = 3.5\% \oplus .42\% \oplus 40MeV/E.$$

The position resolution obtained at 25GeV is 1mm and the time resolution better than 300ps.

3.5. The hadronic calorimeter

The hadronic shower leakage from the LKr calorimeter is measured by a conventional Fe/scintillator calorimeter. It is divided longitudinally into two stacks and contains in total 49 layers of 11.9cm×130cm×.45cm scintillator slabs oriented either horizontally or vertically. The thickness of the hadronic calorimeter corresponds

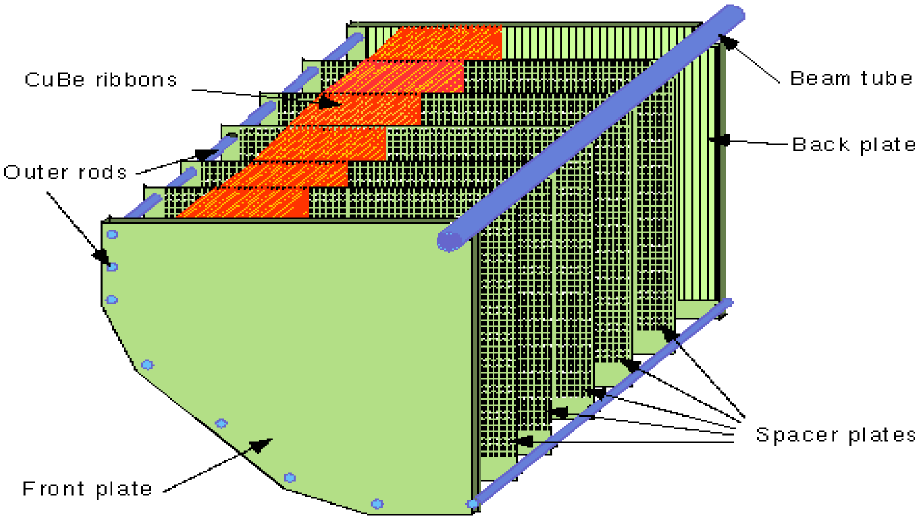

Figure 4. The LKr electrode structure. One fourth of the detector is shown.

to 7.2 interaction lengths and the energy resolution obtained is

$$\frac{\sigma_E}{E} \approx \frac{65\%}{\sqrt{E(GeV)}}.$$

3.6. The muon veto system

The Muon Veto System is made of three layers of NE-110 scintillation counters separated by 80cm of iron. The first two planes have 1cm thick scintillators oriented horizontally and vertically respectively. They are used in the trigger logic to reject $K_{\mu 3}$ decays. The third plane has thinner (6mm) scintillators and is mainly used to monitor the detection efficiency of the first two planes. The efficiency of the Muon Veto System is better than 99% for muons above 5GeV.

4. TRIGGER AND DAQ

The trigger of the experiment is subdivided into different stages of increasing complexity and has been designed to perform at beam intensities 10 times larger than that of the previous generation experiments.

The first level, called "Level 0", makes use of the trigger hodoscopes, the muon veto and the ring anti-counters to deliver within 500ns a fast trigger signal to the following stage. Its rate is below 1MHz at nominal beam intensity.

At the "Level 1" stage, the Neutral Trigger decision derived from the information of the photon detector is available. In a fully pipeline mode, the Neutral Trigger computes the energy in the LKr calorimeter, counts the number of detected peaks in both the x and y projections, computes the centre-of-gravity of the energy deposition as well as the position along the beam axis of the $K^0 \to \pi^0\pi^0$ candidates. It combines also the energy of the hadron calorimeter to provide the total energy of the event. The expected output rate of the Neutral Trigger is less than 2kHz.

The total energy information is used to reduce the rate at the input of the "Level 2" Charged Trigger to about 100kHz. At this stage, the Charged Trigger processes the drift chamber information to compute the vertex and the invariant mass of $K^0 \to \pi^+\pi^-$ candidates. The maximum processing time allowed is 100μs. The output rate of the "Level 2" Charged Trigger is about 1kHz.

Random triggers, calibration triggers as well as downscaled triggers for monitoring purposes can also be provided in parallel by the trigger logic of the experiment.

A "Level 3" stage, not available in 1996, is foreseen to run a complete event reconstruction program on on-line processors so as to keep the total trigger rate below 6kHz.

The event data size is dominated by the LKr calorimeter and depends critically on the suppression of empty channels. The data acquisition system is designed to process 80Mbytes/s at an average rate of 6kHz during 2.4s SPS spills. The total amount of raw data to be put on tape is expected to be 40Tbytes/year.

5. THE 1996 TEST RUN

The 1996 run period was mainly devoted to the installation and commissioning of the LKr calorimeter and to the implementation of the Neutral Trigger in the experiment. Most of the other components of the NA48 detector were already in their final configuration and tested in 1995. A data taking period of 4 days with $K_S + K_L$ beams at nominal intensity took place towards the end of the run for physics studies.

Since only 8% of the LKr electronics was available in 1996, a strategy had to be adopted in order to measure the intrinsic performance of the electromagnetic calorimeter and to study $K^0 \to \pi^0\pi^0$ decays with the detector. In a first step, a calibration of 384 individual $2\times2\text{cm}^2$ instrumented cells with an electron beam was performed at different energies (25, 50 and 100GeV/c). In the second step, the entire calorimeter was read-out by instrumenting "supercells" of 2×8 single cells. In this way, many aspects of the Neutral Trigger could be tested and physics data could be taken with K_S and K_L beams.

The LKr calorimeter was successfully operated at 1500V. The maximum driftime was measured to be 3.5μs in agreement with measurements performed in the laboratory. After a first purification of the liquid krypton, the lifetime of the electrons was found to be greater than 45μs for several weeks without any additional purification. The temperature differences inside the cryostat were measured to be smaller than 0.2°K and were very stable as a function of time.

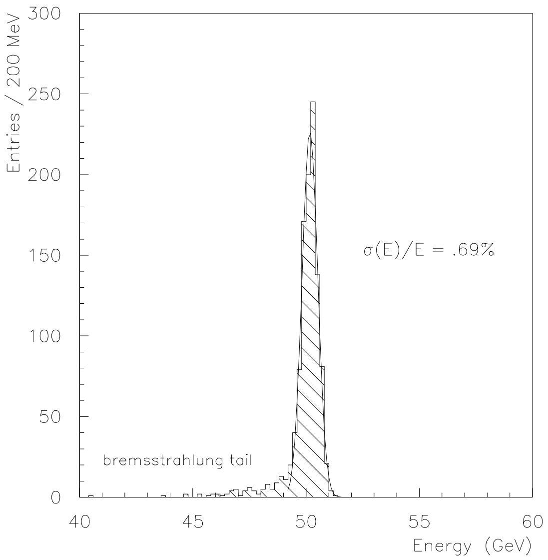

Figure 5. Energy response of the LKr calorimeter to 50 GeV/c electrons.

The performance of the LKr calorimeter was measured during the calibration period with an electron beam. Figure 5 shows the energy deposition in a shower box of 11×11 single cells for 50GeV/c incident electrons. The resolution obtained is .69%, in close agreement with prototype results. The contribution of the noise, dominated by the incoherent component, was less than 8MeV per cell. The low energy tail in the distribution is due to losses in the material in front of the calorimeter. The position resolutions measured at the same energy are 780μm and 970μm in the x and y projections respectively. The time resolution at 100GeV is better than 150ps in the cell containing the maximum energy deposition of the shower.

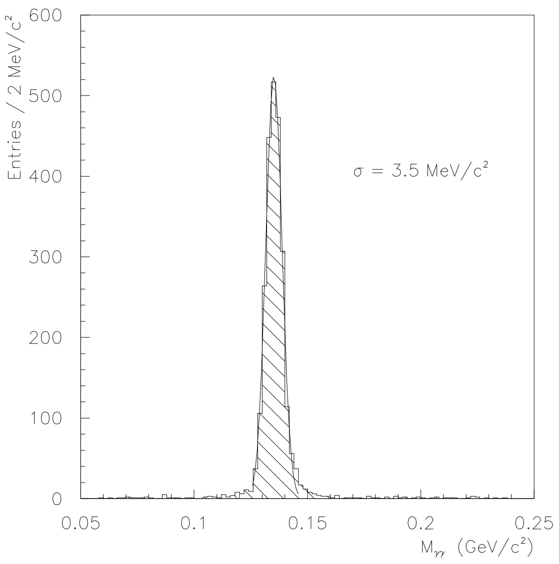

Figure 6. Invariant mass distribution of two photons measured with the LKr calorimeter.

Data taken with the LKr calorimeter fully read out in the "supercell" configuration have permitted to check the different functionalities of the Neutral Trigger. In particular, the total energy and peak counting performed as expected yielding trigger rates slightly above 1kHz. Moreover, $K_{S,L} \to \pi^0\pi^0$ decays with four clusters in the photon detector were clearly identified and their rates were found to agree with the predicted ones. The π^0 mass resolution obtained from 2-body $K_{S,L}$ decays is about 3.5MeV (see figure 6), mainly limited by the poor granularity of the "supercells" and their associated electronic noise. This result is compatible with a mass resolution of about 1MeV that could be reached with instrumented $2 \times 2\text{cm}^2$ single cells.

Very good performances were also obtained with the magnetic spectrometer for the $K_{S,L} \to \pi^+\pi^-$ decays. The four drift chambers worked reliably and provided high detection efficiency and position resolution at rates close to 1MHz. The kaon invariant mass resolution obtained off-line from fully reconstructed $\pi^+\pi^-$ events is 3MeV in both K_S and K_L beams. Moreover, the good resolution on the decay vertex position provides a clear separation of the K_S and K_L sources, allowing a measurement of the tagging efficiency in the charged decay mode.

The Charged Trigger operated satisfactorily in rejecting by a factor of about 70 the 3-body K_L charged decays. The on-line reconstructed kaon mass has a resolution better than 7MeV in $K_S \to \pi^+\pi^-$ decays and the reconstruction efficiency of the trigger is close to 98%.

Analysis of both neutral and charged kaon decays is in progress in order to better understand the performance and acceptance of the NA48 detector, the K_S tagging efficiency and the contributions from several background sources.

6. OUTLOOK AND CONCLUSIONS

The preliminary results of the 1996 test run have indicated that the NA48 detector works according to expectations at nominal $K_S + K_L$ beams intensity. In 1997, the LKr calorimeter will be fully read-out and additional processors for the Charged and Neutral Triggers will be available to cope with higher trigger rates. About 120 days of beam time starting next April are scheduled in 1997. It is expected then to collect more than 10^6 $K_L \to \pi^0\pi^0$ decays superseeding in one year of data taking the statistical precision of the NA31 experiment for the $\Re(\epsilon\prime/\epsilon)$ measurement[?].

REFERENCES

1. G.D. Barr et al., CERN/SPSC/90-22/P253.
2. P. Grafstrom et al., NIM A344 (1994) 487-491.
3. D. Bédérède et al., NIM A367 (1995) 88-91.
4. G.D. Barr et al., NIM A370 (1996) 413-424.
5. G.D. Barr et al., Phys. Lett. B317 (1993) 233-242.